Journal Pre-proof

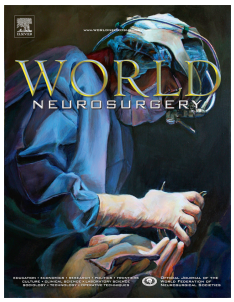

Clinical and MR findings for the diagnosis of recurrent tumors versus radiation-induced secondary tumors of malignant pediatric brain tumors of the posterior fossa

Lo-Yi Lin, Han-Jui Lee, Chia-Hung Wu, Hsin-Wei Wu, Chih-Chun Wu, Kai-Wei Yu, Yi-Wei Chen, Yi-Yen Lee, Hsin-Hung Chen, Jau-Ching Wu, Wei-An Tai, Te-Ming Lin, Feng-Chi Chang

PII: S1878-8750(25)01064-2

DOI: https://doi.org/10.1016/j.wneu.2025.124706

Reference: WNEU 124706

To appear in: *World Neurosurgery*

Received Date: 6 November 2025

Accepted Date: 1 December 2025

Please cite this article as: Lin L-Y, Lee H-J, Wu C-H, Wu H-W, Wu C-C, Yu K-W, Chen Y-W, Lee Y-Y, Chen H-H, Wu J-C, Tai W-A, Lin T-M, Chang F-C, Clinical and MR findings for the diagnosis of recurrent tumors versus radiation-induced secondary tumors of malignant pediatric brain tumors of the posterior fossa, *World Neurosurgery* (2026), doi: https://doi.org/10.1016/j.wneu.2025.124706.

Clinical and MR findings for the diagnosis of recurrent tumors versus radiation-induced secondary tumors of malignant pediatric brain tumors of the posterior fossa

Short title: Radiation-induced 2nd brain tumors

AUTHORS
Lo-Yi Lin [1,2], Han-Jui Lee[1,2], Chia-Hung Wu[1,2,3], Hsin-Wei Wu[1,2], Chih-Chun Wu[1,2], Kai-Wei Yu[1,2], Yi-Wei Chen[2,4,5], Yi-Yen Lee[2,6], Hsin-Hung Chen[2,6], Jau-Ching Wu[2,7,8], Wei-An Tai[1,2], *Te-Ming Lin[1,2], *Feng-Chi Chang [1,2,9]

1 Department of Radiology, Taipei Veterans General Hospital, Taipei, Taiwan
2 School of Medicine, National Yang Ming Chiao Tung University, Taipei, Taiwan
3 Institute of Clinical Medicine, National Yang Ming Chiao Tung University, Taipei, Taiwan
4 Department of Oncology, Taipei Veterans General Hospital, Taipei, Taiwan
5 Department of Medical Imaging and Radiological Technology, Yuanpei University of Medical Technology, Hsinchu City, Taiwan
6 Division of Pediatric Neurosurgery, Department of Neurosurgery, Neurological Institute, Taipei Veterans General Hospital, Taipei, Taiwan
7 Department of Neurosurgery, Neurological Institute, Taipei Veterans General Hospital.
8 Institute of Pharmacology, National Yang-Ming University
9 Neuroscience Research Center, Taipei Medical University Hospital, Taipei, Taiwan

Lo-Yi Lin: zoelin061@gmail.com
Te-Ming Lin: naldo.lin@gmail.com
Feng-Chi Chang: fcchang374@gmail.com

Corresponding author:

Feng-Chi Chang, MD
Department of Radiology, Taipei Veterans General Hospital
201 Sec. 2, Shih-Pai Rd., Taipei 11217 Taiwan
E-mail: fcchang374@gmail.com
Fax: +886-2-28769310
Tel: +886-2-28757031

Te-Ming Lin, MD
Department of Radiology, Taipei Veterans General Hospital
201 Sec. 2, Shih-Pai Rd., Taipei 11217 Taiwan
E-mail: naldo.lin@gmail.com
Fax: +886-2-28769310
Tel: +886-2-28757350

Key words: medulloblastoma; AT/RT; ependymoma; irradiation; second tumor

Clinical and MR findings for the diagnosis of recurrent tumors (RT) versus radiation-induced secondary tumors (RIST) of malignant pediatric brain tumors of the posterior fossa

BACKGROUND

Irradiation is used to treat patients with malignant pediatric brain tumors of the posterior fossa (MPBTPFs)

METHODS

20 MPBTPF patient with RIST (9 benign and 11 malignant)
20 MPBTPF patient with RT

RESULTS

Clinical and MRI features	Malignant RIST vs RT	P value
Latency period	79 vs 22 months	<0.001
Surgical bed	0 % vs 60 %	0.001
Leptomeningeal seeding	0 % vs 45 %	0.01
Tumor volume	23.4 vs 5.2 cm^3	0.004
ADC_{min}	821 vs 644 10^{-6} mm^2/s	0.02
ADC ratio	1.08 vs. 0.96	0.04

CONCLUSION

Radiation induced 2nd tumors and recurrent tumors can be distinguished based on clinical and MRI features

Visual abstract
by Lo-Yi, Lin MD

Abstract

Background: Irradiation is one of the main therapeutic strategies used to treat patients with malignant pediatric brain tumors of the posterior fossa (MPBTPFs). Any recurrent intracranial lesion that forms after treatment completion is either a radiation-induced secondary tumor (RIST) or a recurrent tumor (RT), and patients with these tumors have similar presentations. The aim of our study was to diagnose RIST and RT on the basis of their clinical and MRI features to guiding optimal treatment strategies

Methods: From 2003–2022, we retrospectively enrolled 20 MPBTPF patients with pathologically confirmed RIST after complete surgery and irradiation. We also enrolled 20 MPBTPF patients with RTs with matched primary tumor types and evaluated the clinical and MRI findings and outcomes of these patients.

Results: The latency period was significantly longer in RISTs than in RTs (152.5 vs. 22 months, $p<0.001$). None of the RISTs arose from the primary surgical bed or exhibited leptomeningeal seeding. Benign RISTs tended to be well-defined and showed homogeneous enhancement. In contrast, malignant RISTs largely resembled RTs morphologically but demonstrated larger tumor volumes and higher ADC_{min} and ADC ratios (all $p<0.05$). ROC analysis revealed that latency was the strongest discriminator between malignant RISTs and RTs (AUC=0.90), followed by tumor volume (AUC=0.81), ADCmin (AUC=0.76), and ADC ratio (AUC=0.72)

Conclusion: In patients with MPBTPF who undergo surgery and radiotherapy, RISTs can be distinguished from RTs by clinical and MRI features, which may help guide early treatment planning.

Introduction

Infratentorial tumors account for 45–60% of all pediatric brain tumors. [1] Among them, 30–40% of tumors are medulloblastomas, 25–35% are pilocytic astrocytomas, 20-25% are brainstem gliomas, 10-15% are ependymomas, less than 1-2% are atypical teratoid rhabdoid tumors (ATRTs), and 10-15% of posterior fossa brain tumors represent other histological types. [2] In children, postoperative adjuvant radiotherapy has greatly improved the outcomes of patients with malignant pediatric brain tumors of the posterior fossa (MPBTPFs). [3] However, there is growing concern with respect to the effects of radiotherapy-related complications that affect the neurocognitive, cerebrovascular, visual, and pituitary systems of these children; the delays in growth; and the possibility of developing radiation-induced secondary tumors (RISTs). [4] The following criteria for diagnosing a RIST were developed by Cahan et al. for radiotherapy-induced solid tumors in 1948 [5]: occurrence within the original radiotherapy field, occurrence only after a latency period following radiotherapy; histological distinctness from the original tumor; and no cancer predisposition syndrome present. RISTs include both benign and malignant neoplasms, including meningiomas, high-grade gliomas, and sarcomas. [6]

In addition to RISTs, recurrent tumors (RTs) arising from malignant brain tumors remain the most common cause of mortality in long-term survivors of pediatric brain tumors treated with radiotherapy. In one single-center study, the median latency for local recurrence of medulloblastoma was 25 (11–78) months, and that for supratentorial recurrence was 15 (0–72) months. [7] Sometimes, the residual tumor remains stable for a longer time. One possible explanation is that tumor regrowth is suppressed by radiotherapy.[8] The other possibility is that biological eradication of the tumor is achieved by the initial treatment but that the kinetics of the surrounding cells are altered by the treatment, which leads to a second occurrence of medulloblastoma. [8] These recurrent tumors may manifest as a focal mass lesion, leptomeningeal dissemination or both. If the recurrent tumor develops after a long period and manifests as focal mass lesions, differentiating the tumor from RISTs can be difficult.

For RTs, the standard management is maximal safe re-resection when feasible, followed by consideration of re-irradiation with advanced techniques (such as stereotactic radiosurgery, intensity modulated radiation therapy, or hypofractionated regimens) and/or systemic therapy tailored to the tumor's histology and molecular profile.[9-11] In contrast, for RISTs (such as high-grade glioma, meningioma, or sarcoma), a more cautious approach is warranted due to their distinct biology and heightened risk of radiation-related toxicity. Maximal safe surgical resection remains the mainstay, while adjuvant therapy should be individualized.[6] When additional

radiotherapy is considered, modalities that minimize normal tissue exposure (e.g., proton beam therapy) are preferred, with stricter adherence to cumulative dose constraints. Molecular and genetic profiling is essential, as these tumors often display unique features compared with recurrent primary tumors. Given the higher risk of radiation-induced complications, systemic therapy may be prioritized when local treatment options are limited.[12] In summary, RTs are treated as relapsed disease of the original histology, whereas RISTs are managed as de novo malignancies according to their respective histology, with careful consideration of prior treatment exposures and cumulative toxicity.

This retrospective study was designed to evaluate the clinical and MRI findings of RIST and RT in MPBTPF patients who underwent complete surgery followed by radiotherapy, with the aim of guiding optimal treatment strategies.

Materials and methods

This retrospective study was approved and deemed exempt from the need to obtain individual consent from the patients by the institutional review board of our institute. Informed consent to perform imaging examinations, surgery and adjuvant cancer treatment was obtained from each patient or a member of the patient's family.

Patients

We retrospectively reviewed the charts of consecutive patients with MPBTPF treated with complete operation and adjuvant radiotherapy at our center. RIST was defined as any new neoplasm that arose within the irradiated field with a pathological diagnosis that differed from that of the primary tumor. RT was defined as a neoplasm with the same pathological diagnosis as the primary malignancy. From July 2003 to September 2022, among 256 patients with posttreatment MPBTPF at our center, a total of 20 patients with pathologically proven RIST were enrolled in this study. None of the enrolled patients had a cancer predisposition syndrome. For the RT group, we attempted to match the primary tumor types and age in the RIST group (15 medulloblastomas, 4 ATRTs, and 1 ependymoma). However, pathologically confirmed recurrent medulloblastoma and ATRT were uncommon (12 medulloblastomas and 3 ATRTs in total during this period). Therefore, 5 additional ependymomas were included (7 ependymomas in total). There was no significant difference in the distribution of primary tumor types between the two groups ($p = 0.21$). The demographic features and clinical findings of both groups were analyzed.

MRI before reoperation

The MRI machines used were 1.5 T systems (Siemens Medical Solutions; GE Medical Systems; or Philips Medical Systems). The MRI examination included axial T1WI, T2WI, and DWI with b values of 0 and 1000 s/mm2, ADC maps generated automatically by the MRI scanners, and contrast-enhanced T1WI of the brain. All patients underwent a complete MR imaging study before reoperation. The MR imaging parameters of the mass lesion were analyzed by neuroradiologists without knowledge of the final reoperative pathology.

These parameters included the following: (1) T1WI, T2WI, and DWI signal intensities with the ADC, classified as iso-to-high or low signal intensity (SI) compared with signals from the adjacent normal white matter of the brain; restricted diffusion, defined as high SI on DWI and low SI on ADC in comparison with the adjacent normal white matter. Enhancement on contrast-enhanced T1WI was classified as homogenous or heterogenous, and a as “good” when the strongest focal signal intensity was comparable to that of adjacent venous structures, as “faint” when

the enhancing signals were weaker than the venous structures, and as "no enhancement" when the lesion was not brighter than on the precontrast images.

(2) Absolute ADC values (ADC_{min}) were measured by manually positioning regions of interest (ROIs) that were 10–50 mm^2 in size on the hospital's picture archiving and communication system (PACS) workstations. The tumor ROIs were positioned on the homologous area with the lowest signals within the solid components while avoiding areas with necrosis, peritumoral edema, calcification and hemorrhage. If the tumor appeared in more than three images (slice thickness 5 mm), three ROIs were placed on different sections and subsequently averaged. If the tumor appeared in fewer than three images, a total of three ROIs were placed within the tumor to avoid overlap. To offset subtle differences in the signal settings of different MRI scanners, an additional ROI was positioned on the homologous area of normal-appearing contralateral white matter in the cerebrum or cerebellum. The ADC ratio was calculated as the solid tumor-to-contralateral white matter ratio. We suggest the ADC ratio is able to reduce some factors related to imaging artifact or imaging inhomogeneity by different MR scanners. The DWI ratios (b = 1000 s/mm2) were obtained in a similar manner but by positioning the tumor ROIs at areas with the highest signals.

(3) Information on the following diagnostic variables was obtained: tumor volume, which was estimated using the geometric ellipsoid formula. Specifically, the three orthogonal maximum diameters of the tumor (length, width, and height) were measured on MRI, and the volume was calculated as:

$$V = \frac{\pi}{6} \times length \times width \times height$$

Tumor location, at the primary tumor base or distal to the primary tumor; tumor margin, categorized as well-defined or poorly defined; the presence of a cystic component or complete solid component; peritumoral edema; the presence of tumor seeding; and the presence of hydrocephalus.

Two neuroradiologists, each with 3 and 27 years of experience, evaluated the imaging parameters, and decisions were made by consensus.

Statistical analysis

To evaluate the associations between the clinical and MRI parameters in the RIST and RT groups, numeric and continuous data, such as data on patient age, tumor size, latency period, ADC_{min}, the ADC ratio, and the DWI ratio, are summarized as the median values and were analyzed with Mann-Whitney U test. Categorical data, such

as data pertaining to sex, tumor location, tumor margin and MRI parameters, are summarized as counts and percentages and were analyzed with a chi-square test or Fisher's exact test, with the analysis results presented as p values.

Calculation of the area under the receiver operating characteristic (ROC) curve (AUC) was performed to assess the diagnostic accuracy of imaging parameters showing significant differences. The optimal cutoff levels of the latency, tumor volume, ADC_{min} and ADC ratio for differentiating between malignant RIST and RT were analyzed by means of ROC curves and Youden's index. Kaplan–Meier plots were used to visualize data on overall survival (OS) following a RIST or RT diagnosis, and between-group comparisons of OS were analyzed by means of the log-rank test. All the statistical analyses were performed with IBM® SPSS® software, and P values <0.05 indicated statistical significance.

Results

Clinical characteristics of the patients with RISTs

In total, 20 patients developed RISTs following cranial radiotherapy for MPBTPF (Table 1). There were 13 female patients and 7 male patients, and the median age at first radiotherapy was 7 years (range, 1–14 years). The MPBTPFs included the following: medulloblastoma (n=15), ATRTs (n=4), and ependymoma (n=1). RISTs developed after a median latency period of 152.5 months (range, 34–400 months). The 20 RISTs included meningioma (n=8, 40%), glioblastoma (GBM) (n=7, 35%), high-grade astrocytic neoplasm (n=1, 5%), malignant spindle cell tumor (n=1, 5%), osteosarcoma (n=1, 5%), olfactory neuroblastoma (n=1, 5%), and trigeminal schwannoma (n=1, 5%). None of the RISTs grew on the primary tumor surgical bed. The follow-up period, measured from the diagnosis of the primary tumor until death or last follow-up, showed that the median follow-up for benign RIST was 392 months (205–492 months), and for malignant RIST it was 89 months (55–345 months).

Clinical findings of the RIST and RT

The results of the comparisons of the clinical findings in the RIST and RT groups are presented in Table 2. The primary tumors in the RT group were medulloblastoma (n=12, 60%), ATRT (n=3, 15%) and ependymoma (n=5, 25%). The latency period between initial surgery and reoperation was 152.5 months (range, 34–400 months) in the RIST group and 22 (1–191) months in the RT group ($P<0.001$). The median follow-up for RT was 43.5 months (6–209 months). The age at diagnosis of the primary tumor, sex, and number of patients who were alive at the last follow-up were not significantly different between the two groups.

OS analysis revealed that the OS times of the patients with benign RISTs (median OS >200 months) were better than those of the patients with RT (median OS= 22 months) ($p=0.04$). There were no significant differences in the median OS times of all patients with RISTs (median OS= 30 months) versus patients with RTs (median OS= 22 months), of patients with malignant RISTs (median OS= 12) versus patients with RTs (median OS= 22 months), or between patients with benign RISTs (median OS >200 months) and patients with malignant RISTs (median OS= 12). (Figure 1)

MRI characteristics by tumor group (Table 3)

Malignant RIST vs. RT

Pre-reoperation, no malignant RIST arose at the primary surgical bed (0/11), whereas 12/20 RTs were at the surgical bed (60%; $p=0.001$). Tumor volume was larger in malignant RISTs [23.39 cm^3 (2.72–57.4) vs 5.17 cm^3 (0.21–63.54);

p=0.004]. CSF seeding was absent in malignant RISTs but present in 9/20 RTs (45%; p=0.01). Diffusion metrics also differed: ADC_{min} was higher [821×10^{-6} mm²/s (638–1392) vs 644×10^{-6} mm²/s (64–1208); p=0.02], and the tumor-to-normal ADC ratio was greater [1.08 (0.81–2.71) vs 0.96 (0.70–1.87); p=0.04]. No significant between-group differences were found for lesion margin definition, T1/T2 signal characteristics, overall enhancement intensity or pattern, presence of a cystic component, perifocal edema, hydrocephalus, diffusion restriction on DWI, or DWI ratio (all p>0.05).

Benign RIST vs. RT

Pre-reoperation, no benign RIST arose at the primary surgical bed (0/9), whereas 12/20 RTs were at the surgical bed (60%; p=0.003). Benign RISTs were predominantly extra-axial (8/9, 89%), while more RTs were intra-axial (11/20, 55%; p=0.04). Lesion margins were more often well-defined (9/9, 100% vs 3/20, 15%; p<0.001), and homogeneous enhancement was more common (8/9, 89% vs 2/20, 10%; p<0.001). CSF seeding was absent in benign RISTs but present in 9/20 RTs (45%; p=0.03). Diffusion metrics differed: the tumor-to-normal ADC ratio was higher [1.15 (0.90–1.82) vs 0.96 (0.71–1.87); p=0.03], and the DWI ratio was lower [1.22 (0.76–1.37) vs 1.43 (0.85–1.71); p=0.01]. Tumor volumes were comparable [2.35 cm³ (0.99–174.37) vs 5.17 cm³ (0.21–63.54); p=0.62]. Other MRI features did not differ (all p>0.05).

Benign RIST vs. Malignant RIST

All lesions in both groups were distant from the primary surgical bed (100% each; p=1). Benign RISTs were more often extra-axial (8/9, 89%) than malignant RISTs (2/11, 18%; p=0.01) and more frequently well-defined (9/9, 100% vs 3/11, 27%; p=0.001). Homogeneous enhancement was also more common in benign RISTs (8/9, 89%) than in malignant RISTs (3/11, 27%; p=0.01). Tumor volume was smaller in benign RISTs [2.35 cm³ (0.99–174.37)] than in malignant RISTs [23.39 cm³ (2.72–57.4); p=0.007]. Other MRI features did not differ (all p>0.05).

In summary, across all RIST cases, no tumors arose in the primary tumor's surgical bed. RISTs occurred in both extra- and intra-axial locations, whereas every tumor in the RT cohort was intra-axial. None of the RISTs showed CSF seeding, which was observed in the RT group. Compared with RT, benign RISTs differed in several anatomic and morphologic characteristics—most notably in margin definition and enhancement pattern. By contrast, malignant RISTs and RT shared broadly similar anatomic/morphologic features; however, malignant RISTs tended to have larger

tumor volumes and higher ADC_{min} and ADC ratio than RT, providing useful clues for differentiation. The MRI features of malignant RIST and RT are presented in Figure2.

ROC analysis

In differentiating malignant RIST from RT, ROC analysis demonstrated that latency, tumor volume, ADC_{min}, ADC value provided discriminatory value (Figure 3). Latency yielded the highest accuracy (AUC = 0.90; 95% CI, 0.78–1.00) with an optimal cut-point of 33 months (sensitivity 100%, specificity 75%). Tumor volume showed acceptable performance (AUC = 0.81; 95% CI, 0.67–0.97) with an optimal cut-point of 12.1 cm^3 (sensitivity 91%, specificity 80%).

Among diffusion metrics, ADC_{min} and the ADC ratio showed fair discrimination, with AUCs of 0.76 (95% CI, 0.59–0.93) and 0.72 (95% CI, 0.52–0.93), respectively. The optimal threshold for detecting RIST was an $ADC_{min} > 692.5 \times 10^{-6}$ mm^2/s (sensitivity 82%, specificity 75%) and an ADC ratio > 1.03 (sensitivity 73%, specificity 80%).

Discussion

In the current study, we demonstrated that clinical and MR findings can be used for the pretreatment diagnosis of benign RIST, malignant RIST, and RT in MPBTPF patients after completion of initial surgery and radiotherapy. Compared with RT patients, the latency period is longer in both benign and malignant RIST patients. Furthermore, all RISTs do not grow on the surgical bed of the primary tumor, do not have concurrent leptomeningeal seeding, and have a more extra-axial position. Benign RISTs show more well-defined margins and homogeneous enhancement than RTs. Although malignant RISTs often exhibit ill-defined margins and heterogeneous enhancement similar to RTs, they tend to have larger tumor volumes and higher ADC_{min} and ADC ratios, which help distinguish them from RTs. Compared with that for RT patients, the OS of patients with benign RISTs is better. To date, this is the largest series in which MR image analysis for RISTs after surgery and radiotherapy was evaluated for pediatric MPBTPF. We also provide a flow chart for differential RISTs and RTs, shown in Figure 4.

Applications and risks of radiotherapy in MPBTPF

In addition to surgery, radiotherapy is one of the main treatment modalities used to improve the survival outcomes of MPBTPF patients. [3] Currently, children aged > 2 years who have undergone gross total resection of their medulloblastomas with no evidence of CNS dissemination at diagnosis (average risk) are conventionally treated with 23.4 Gy of craniospinal irradiation (CSI) with concomitant vincristine and 32.4 Gy posterior fossa radiation therapy, followed by adjuvant cis-platinum–based chemotherapy. [13] Patients with ependymomas receive a higher radiotherapy dose, with ACNS0121 recommending 54 Gy for patients aged < 12–18 months after gross total resection and 59.4 Gy for all other patients. [14] Radiotherapy affects tumors by causing DNA damage, specifically double-strand breaks. However, DNA damage also occurs in healthy cells that are exposed to radiotherapy. Tremendous progress has been made over time to limit both the dose and field of radiation exposure to minimize damage to healthy cells. [13] Despite the advancements in radiotherapy methods, some degree of inherent risk, which can lead to neurological deficits in 45.5% of patients [15] and cause RIST in 1–4% of patients, remains. [16, 17] In previous studies, the types of RISTs were mainly meningiomas, malignant gliomas, nerve sheath tumors, secondary squamous cell carcinomas and sarcomas. [18] In our study, meningioma and high-grade glioma were the most common RISTs and accounted for 80% of all cases, consistent with the findings of previous studies.

Risk of secondary tumors

A widely held concept is that the younger the patient is at primary treatment, the greater the risk of RIST will be. Lee et al. reported that age at irradiation of <7 years and craniospinal irradiation significantly increased the risk of developing a secondary tumor. [6] Younger onset may therefore render patients especially vulnerable to radiation-induced gliomagenesis in later years due to the abundance of neurogenic stem cells and increased growth factor activity. [19] Paulino et al. reported that children undergoing prophylactic cranial irradiation in the management of acute leukemias constitute the largest risk group. [20] They also reported that the radiotherapy volume affected the latency time. In patients receiving craniospinal or whole-brain irradiation, 72.5% of the RIGs occurred within 10 years of initial radiotherapy. In those treated with local irradiation, 51.2% of the RIGs occurred within 10 years of radiotherapy. [20] Lee et al. also reported a higher incidence of secondary tumors in those with primary medulloblastomas. [6] For patients with medulloblastoma who should receive craniospinal irradiation according to the previous standard protocol, selective dose de-escalation or focal irradiation for favorable genotypes, such as wingless (WNT)-subgroup medulloblastoma, may be considered. [21]

Latency of secondary tumors

In their article, Pettorini et al. [22] reviewed 142 tumors in patients who received irradiation of the whole CNS in childhood; they reported mean latency periods of 13.7 years for secondary meningioma and 7.5 years for secondary sarcoma. The latency period for development a RIG ranges from 9 to 11 years. [4, 23] Aherne et al revealed that the latency period of WHO grade II-VI RIGs was approximately 10.7 to 12.6 years. [24] Among our patients, the median latency period was 21.5 (8 to 33.3) years for benign RISTs, including 8 meningiomas, and 6.6 (2.8 to 20.8) years for malignant RISTs, including 7 GBMs. Our latency periods for RISTs were consistent with those of reported in other series. In our study, RIST may have occurred with a longer interval than RT after cranial radiotherapy, especially for benign RISTs, warranting extended long-term follow-up of exposed patients.

Outcome of secondary tumors

In one cohort study, 1–4% of patients who underwent cranial radiotherapy for pediatric cancer developed radiation-induced gliomas (RIGs), and among them, 56.1% of the RIGs were WHO grades 3–4, and 43.9% of them were WHO grades 1–2. At one year post-RIG diagnosis, overall survival (OS) was 44.5%, two-year OS was 15.9%, 3-year OS was 6.4%, and the median OS was 9.0 months. [17] A meta-

analysis of 296 cases of radiation-induced gliomas reported a median overall survival of 11 months (95% CI, 9–12 months) and a 2-year survival rate of 20.2% across all grades, with most secondary gliomas being high-grade (grade III/IV) tumors.[25] In our study, the incidence of RIG was 3.1%, consistent with the findings in the above study, and the median OS among patients with malignant RISTs was 12 months, consistent with the findings of previous studies. In our study, the outcomes of the patients with malignant RISTs were similar to those of the patients with RTs. However, patients with benign RISTs had better outcomes than those with RTs (median OS>200 and 22 months, respectively, p=0,04).

Treatment for secondary tumors

Treatment for RIG remains less standardized as compared with that of primary gliomas. Patients with RIG have poor responses to chemotherapy. Reirradiation is an option in selected patients. Paulino et al. reported that 85 patients with RIG who received reirradiation at a median dose of 50 Gy had higher 1-, 2-, and 5-year survival rates than those who did not undergo reirradiation treatment. [20] Surgical resection may increase the OS time [26], but overall, the patient outcomes are largely poor. Leary et al. reported that regardless of the type of treatment, including surgery, chemotherapy, or radiation, there were no significant differences in median OS between groups who did or did not receive treatment. [17] In our study, all patients with RIST underwent surgery. Among the 9 benign RIST cases (8 meningiomas and 1 trigeminal schwannoma), 2 meningiomas additionally received gamma knife radiosurgery. Of the 8 secondary high-grade gliomas, 2 received RT, 3 received concurrent chemoradiotherapy (CCRT), and 3 underwent CCRT combined with targeted therapy and boron neutron capture therapy (BNCT). For other malignant RISTs, the olfactory neuroblastoma case received CCRT, the osteosarcoma case received chemotherapy, and the malignant spindle cell tumor case received radiotherapy. However, the outcomes of malignant RIST were still poor, with a median OS of only 12 months.

Imaging features for differentiating RIST from RT

Patients with recurrent posterior fossa malignancies may present with focal mass lesions, leptomeningeal dissemination or both. If recurrent MPBTPFs develop after a long period and manifest as focal mass lesions, they may be difficult to differentiate from RISTs in an imaging study. In the current study, we were able to differentiate RIST of the MPBTPF from RT in an MR imaging study. The features included the following:

1. Lesion location. RTs may develop from small unresected or invisible residual tumors within or close to the surgical tumor bed. However, in RISTs, DNA damage occurs in all healthy cells exposed to radiotherapy rather than in the original surgical bed alone. In our study, all the RISTs grew in locations that were distal to the surgical tumor bed; in contrast, 40% of the RTs grew in locations distal to the surgical bed, and the other 60% of the RTs grew on the surgical bed. The radiotherapy area includes extracranial structures, such as the cranial nerves, dura matter, skull bone or scalp. Among our 20 patients with RISTs, 11 (55%) had extra-axial RISTs (8 meningiomas from dura matter, 1 olfactory neuroblastoma from olfactory nerve, 1 osteosarcoma from skull, 1 malignant spindle cell tumor from skin). In contrast, within the RT group, 11 patients had focal intra-axial tumors, while the remaining 9 patients exhibited both leptomeningeal seeding and focal intra-axial tumors. None of the RTs originated from extracranial structures.
2. Subtle leptomeningeal enhancement. Leptomeningeal recurrence or seeding is most commonly detected in patients with medulloblastoma [27] but is also observed in patients with tumors with other pathologies, including ATRT [28] and ependymoma [29]. Our RT group included 12 patients with recurrent medulloblastoma, 3 with recurrent ATRT, and 5 with recurrent ependymoma, and leptomeningeal dissemination is more common with these tumor types than with RISTs (meningioma, high-grade glioma). In our patients, half of these subtle leptomeningeal enhancements on early postprocedural MRI resulted in leptomeningeal recurrence.
3. Lesion margin and enhancement. Meningiomas account for most benign RISTs. A critical difference between radiotherapy-induced meningiomas and sporadic meningiomas is their clinical behavior. In some studies, the rate of more aggressive pathologic subtypes in radiotherapy-induced meningiomas was reported to be higher than that in sporadic meningiomas. [27] In the 8 meningiomas in our RIST group, all had unfavorable features, such as a significant mass effect on adjacent structures, rapid interval growth, and the need for surgical resection. However, these meningiomas still retain their typical MRI and pathological features, leading to more well-defined margins and homogenous enhancement of benign RISTs than of RTs.
4. DWI and the ADC value. Tumors classified as WHO grade IV, such as medulloblastoma and glioblastoma, have the lowest ADC values and ADC ratios because of their high cellularity. Hassannejad E et al. reported that there is no difference in the ADC values of medulloblastoma and glioblastoma. [30] However, the most common malignant RIST “high grade gliomas” include not only WHO grade IV glioblastoma but also WHO grade III anaplastic astrocytoma.

Yamasaki et al. reported a significant inverse relationship between the ADC and astrocytic tumors of WHO grade III vs. IV ($p < 0.01$). [31] Furthermore, high-grade gliomas may have higher ADC values as a result of microcystic degeneration, foci of necrosis, and excessive production of extracellular matrix components by glioblastoma cells. [32] This could explain our finding that the ADC_{min} and ADC ratio were higher in malignant RISTs (mainly high-grade gliomas) than in RTs (including recurrent medulloblastoma, ATRT and ependymoma).

Limitation

The present study had certain limitations. First, this was a retrospective study that included a small number of cases. Second, the therapeutic protocols and irradiation techniques changed during long-term follow-up, extending beyond 20 years in some cases. Given the long follow-up period, the tumor classifications likely span multiple versions of the WHO criteria, making it difficult to confirm that each case meets the most recent standards. For consistency, we uniformly use the term ‘glioblastoma (GBM)’ for cases previously diagnosed as glioblastoma multiforme, ‘ependymoma’ for cases previously classified as anaplastic ependymoma, and ‘astrocytoma’ for cases previously described as anaplastic oligoastrocytoma.

However, RISTs that occur after surgery and radiotherapy in pediatric patients with MPBTPF are rare, and this is the first study in which the MRI features of these tumors are reviewed. Thus, a study of 20 cases of RIST can still provide a valuable reference for understanding the characteristics of this disease. New techniques, such as MRI perfusion and MR spectroscopy, can be used as adjuvant protocols for the early-stage diagnosis of RIST or RT. Further multicenter, prospective studies should also be performed to elucidate the behaviors and characteristics of RIST of MPBTPF.

Conclusion

RISTs and RTs can sometimes appear similar on MRI. In our study, all RISTs had a longer latency period, did not arise at the primary tumor bed, and were not associated with leptomeningeal dissemination. Benign RISTs tended to be well-defined and showed homogeneous enhancement. Malignant RISTs largely resembled RTs morphologically but demonstrated larger tumor volumes and higher ADC_{min} and ADC ratios. Patients with benign RISTs had better outcomes than those with RTs. Therefore, distinguishing between benign RISTs, malignant RISTs, and RTs is crucial for predicting patient outcomes and selecting the most appropriate treatment strategies.

Funding sources

This study has received funding from Taipei Veterans General Hospital, Taiwan [V114C-034, V112B-007 (to CHW); V114C-061,V113C-182, V112C-059, V112D67-002-MY3-3, V112D67-002-MY3-2, V112D67-002-MY3-1 (to FCC)], Veterans General Hospitals and University System of Taiwan Joint Research Program [VGHUST 110-G1-5-2 (to FCC)], National Science and Technology Council, Taiwan [NSTC 111-2314-B-075-025-MY3 and 110-2314-B-075-005- (to CHW); 113-2314-B-075-037-,112-2314-B-075-066- and 110-2314-B-075-032, (to FCC)], Vivian W. Yen Neurological Foundation (to CHW and FCC)

1. Rickert CH, Paulus W. Epidemiology of central nervous system tumors in childhood and adolescence based on the new WHO classification. Childs Nerv Syst. 2001;17(9):503-11. doi: 10.1007/s003810100496. PubMed PMID: 11585322.
2. Kerleroux B, Cottier JP, Janot K, Listrat A, Sirinelli D, Morel B. Posterior fossa tumors in children: Radiological tips & tricks in the age of genomic tumor classification and advance MR technology. J Neuroradiol. 2020;47(1):46-53. Epub 20190918. doi: 10.1016/j.neurad.2019.08.002. PubMed PMID: 31541639.
3. Muzumdar D, Ventureyra EC. Treatment of posterior fossa tumors in children. Expert Rev Neurother. 2010;10(4):525-46. doi: 10.1586/ern.10.28. PubMed PMID: 20367206.
4. Nishio S, Morioka T, Inamura T, Takeshita I, Fukui M, Sasaki M, et al. Radiation-induced brain tumours: potential late complications of radiation therapy for brain tumours. Acta Neurochir (Wien). 1998;140(8):763-70. doi: 10.1007/s007010050177. PubMed PMID: 9810442.
5. Cahan WG, Woodard HQ, et al. Sarcoma arising in irradiated bone; report of 11 cases. Cancer. 1948;1(1):3-29. doi: 10.1002/1097-0142(194805)1:1<3::aid-cncr2820010103>3.0.co;2-7. PubMed PMID: 18867438.
6. Lee CY, Chen YW, Lee YY, Chang FC, Chen HH, Lin SC, et al. Irradiation-Induced Secondary Tumors following Pediatric Central Nervous System Tumors: Experiences of a Single Institute in Taiwan (1975-2013). Int J Radiat Oncol Biol Phys. 2018;101(5):1243-52. Epub 20180424. doi: 10.1016/j.ijrobp.2018.04.032. PubMed PMID: 29859788.
7. Sure U, Bertalanffy H, Isenmann S, Brandner S, Berghorn WJ, Seeger W, et al. Secondary manifestation of medulloblastoma: metastases and local recurrences in 66 patients. Acta Neurochir (Wien). 1995;136(3-4):117-26. doi: 10.1007/BF01410612. PubMed PMID: 8748840.
8. Amagasaki K, Yamazaki H, Koizumi H, Hashizume K, Sasaguchi N. Recurrence of medulloblastoma 19 years after the initial diagnosis. Childs Nerv Syst. 1999;15(9):482-5. doi: 10.1007/s003810050444. PubMed PMID: 10502011.
9. De Pietro R, Zaccaro L, Marampon F, Tini P, De Felice F, Minniti G. The evolving role of reirradiation in the management of recurrent brain tumors. J Neurooncol. 2023;164(2):271-86. Epub 20230825. doi: 10.1007/s11060-023-04407-2. PubMed PMID: 37624529; PubMed Central PMCID: PMCPMC10522742.
10. Bakst RL, Dunkel IJ, Gilheeney S, Khakoo Y, Becher O, Souweidane MM, et al. Reirradiation for recurrent medulloblastoma. Cancer. 2011;117(21):4977-82. Epub 20110414. doi: 10.1002/cncr.26148. PubMed PMID: 21495027.
11. Graen P, Christiansen H, Polemikos M, Heetfeld C, Feuerhake F, Wiese B, et al. Moderately Hypofractionated Radio(chemo)therapy With Simultaneous Integrated

Boost for Recurrent, Previously Irradiated, High-grade Glioma. Anticancer Res. 2023;43(5):2155-60. doi: 10.21873/anticanres.16377. PubMed PMID: 37097672.
12. Jiwei B, Abulimiti M, Yonglong J, Jie W, Shuyan Z, Chao L, et al. Proton beam therapy in a patient with secondary glioblastoma (32 years after postoperative irradiation of medulloblastoma): case report and literature review. Radiat Oncol. 2024;19(1):136. Epub 20241005. doi: 10.1186/s13014-024-02515-5. PubMed PMID: 39369243; PubMed Central PMCID: PMCPMC11453085.
13. Michalski JM, Janss AJ, Vezina LG, Smith KS, Billups CA, Burger PC, et al. Children's Oncology Group Phase III Trial of Reduced-Dose and Reduced-Volume Radiotherapy With Chemotherapy for Newly Diagnosed Average-Risk Medulloblastoma. J Clin Oncol. 2021;39(24):2685-97. Epub 20210610. doi: 10.1200/JCO.20.02730. PubMed PMID: 34110925; PubMed Central PMCID: PMCPMC8376317.
14. Merchant TE, Bendel AE, Sabin ND, Burger PC, Shaw DW, Chang E, et al. Conformal Radiation Therapy for Pediatric Ependymoma, Chemotherapy for Incompletely Resected Ependymoma, and Observation for Completely Resected, Supratentorial Ependymoma. J Clin Oncol. 2019;37(12):974-83. Epub 20190227. doi: 10.1200/JCO.18.01765. PubMed PMID: 30811284; PubMed Central PMCID: PMCPMC7186586.
15. Elyan N, Schwenkenbecher P, Grote-Levi L, Becker JN, Merten R, Christiansen H, et al. Radiotherapy in patients with brain metastases with and without concomitant immunotherapy: comparison of patient outcome and neurotoxicity. Discov Oncol. 2024;15(1):656. Epub 20241115. doi: 10.1007/s12672-024-01560-6. PubMed PMID: 39546075; PubMed Central PMCID: PMCPMC11568079.
16. Metselaar DS, du Chatinier A, Stuiver I, Kaspers GJL, Hulleman E. Radiosensitization in Pediatric High-Grade Glioma: Targets, Resistance and Developments. Front Oncol. 2021;11:662209. Epub 20210401. doi: 10.3389/fonc.2021.662209. PubMed PMID: 33869066; PubMed Central PMCID: PMCPMC8047603.
17. Leary JB, Anderson-Mellies A, Green AL. Population-based analysis of radiation-induced gliomas after cranial radiotherapy for childhood cancers. Neurooncol Adv. 2022;4(1):vdac159. Epub 20221003. doi: 10.1093/noajnl/vdac159. PubMed PMID: 36382107; PubMed Central PMCID: PMCPMC9639354.
18. Khanna L, Prasad SR, Yedururi S, Parameswaran AM, Marcal LP, Sandrasegaran K, et al. Second Malignancies after Radiation Therapy: Update on Pathogenesis and Cross-sectional Imaging Findings. Radiographics. 2021;41(3):876-94. Epub 20210423. doi: 10.1148/rg.2021200171. PubMed PMID: 33891523.
19. Tubiana M. Can we reduce the incidence of second primary malignancies

occurring after radiotherapy? A critical review. Radiother Oncol. 2009;91(1):4-15; discussion 1-3. Epub 20090205. doi: 10.1016/j.radonc.2008.12.016. PubMed PMID: 19201045.

20. Paulino AC, Mai WY, Chintagumpala M, Taher A, Teh BS. Radiation-induced malignant gliomas: is there a role for reirradiation? Int J Radiat Oncol Biol Phys. 2008;71(5):1381-7. Epub 20080211. doi: 10.1016/j.ijrobp.2007.12.018. PubMed PMID: 18262733.

21. Henrich N, Marra CA, Gastonguay L, Mabbott D, Malkin D, Fryer C, et al. De-escalation of therapy for pediatric medulloblastoma: trade-offs between quality of life and survival. Pediatr Blood Cancer. 2014;61(7):1300-4. Epub 20140224. doi: 10.1002/pbc.24990. PubMed PMID: 24616367.

22. Pettorini BL, Park YS, Caldarelli M, Massimi L, Tamburrini G, Di Rocco C. Radiation-induced brain tumours after central nervous system irradiation in childhood: a review. Childs Nerv Syst. 2008;24(7):793-805. Epub 20080408. doi: 10.1007/s00381-008-0631-7. PubMed PMID: 18392837.

23. Kaschten B, Flandroy P, Reznik M, Hainaut H, Stevenaert A. Radiation-induced gliosarcoma. Case report and review of the literature. J Neurosurg. 1995;83(1):154-62. doi: 10.3171/jns.1995.83.1.0154. PubMed PMID: 7782835.

24. Aherne NJ, Murphy BM. Radiation-Induced Gliomas. Crit Rev Oncog. 2018;23(1-2):113-8. doi: 10.1615/CritRevOncog.2018025740. PubMed PMID: 29953370.

25. Yamanaka R, Hayano A, Kanayama T. Radiation-induced gliomas: a comprehensive review and meta-analysis. Neurosurg Rev. 2018;41(3):719-31. Epub 20161005. doi: 10.1007/s10143-016-0786-8. PubMed PMID: 27709409.

26. Carret AS, Tabori U, Crooks B, Hukin J, Odame I, Johnston DL, et al. Outcome of secondary high-grade glioma in children previously treated for a malignant condition: a study of the Canadian Pediatric Brain Tumour Consortium. Radiother Oncol. 2006;81(1):33-8. Epub 20060914. doi: 10.1016/j.radonc.2006.08.005. PubMed PMID: 16973227.

27. Abrey LE, Chamberlain MC, Engelhard HH. Leptomeningeal metastases. New York: Springer Science; 2005. vi, 196 p. p.

28. Parmar H, Hawkins C, Bouffet E, Rutka J, Shroff M. Imaging findings in primary intracranial atypical teratoid/rhabdoid tumors. Pediatr Radiol. 2006;36(2):126-32. Epub 20051208. doi: 10.1007/s00247-005-0037-6. PubMed PMID: 16341528.

29. Qian X, Goumnerova LC, De Girolami U, Cibas ES. Cerebrospinal fluid cytology in patients with ependymoma: a bi-institutional retrospective study. Cancer. 2008;114(5):307-14. doi: 10.1002/cncr.23799. PubMed PMID: 18698591.

30. Hassannejad E, Mohammadifard M, Payandeh A, Bijari B, Shoja A, Abdollahi M, et al. Correlation of ADC values of adult brain tumors with the diagnosis and

pathological grade: A cross-sectional multicenter study. Health Sci Rep. 2024;7(6):e2110. Epub 20240604. doi: 10.1002/hsr2.2110. PubMed PMID: 38841116; PubMed Central PMCID: PMCPMC11150419.

31. Fumiyuki Yamasaki KK, Kenichi Satoh, Kazunori Arita, Kazuhiko Sugiyama, Megu Ohtaki, Junko Takaba, Atushi Tominaga, Ryosuke Hanaya, Hiroyuki Yoshioka, Seiji Hama, Yoko Ito, Yoshinori Kajiwara, Kaita Yahara, Taiichi Saito, Muhamad A Thohar. Apparent diffusion coefficient of human brain tumors at MR imaging. Radiology. 2005;Jun;235(3):985-91. doi: DOI: 10.1148/radiol.2353031338. PubMed Central PMCID: PMC15833979.

32. Tsougos I, Svolos P, Kousi E, Fountas K, Theodorou K, Fezoulidis I, et al. Differentiation of glioblastoma multiforme from metastatic brain tumor using proton magnetic resonance spectroscopy, diffusion and perfusion metrics at 3 T. Cancer Imaging. 2012;12(3):423-36. Epub 20121026. doi: 10.1102/1470-7330.2012.0038. PubMed PMID: 23108208; PubMed Central PMCID: PMCPMC3494384.

Figure 1. (A) Overall survival (OS) for RIST vs RT. (B) OS for benign RIST vs RT. (C) OS for malignant RIST vs RT. (D) OS for benign vs malignant RIST. Only the comparison between benign RIST and RT was statistically significant.

Figure 2. A and B show a patient with malignant RIST (glioblastoma), and C and D show a patient with RT (recurrent medulloblastoma). Both patients had previously undergone surgery and radiotherapy for posterior fossa medulloblastoma. (A, C) At 137 and 191 months after the initial treatment, respectively, both patients developed ill-defined, heterogeneous intra-axial tumors located away from the prior surgical bed. (B) The malignant RIST (glioblastoma) had an ADC_{min} of 1,207 × 10^−6 mm^2/s and an ADC ratio of 1.48. (D) The recurrent medulloblastoma had an ADC_{min} of 680 × 10^−6 mm^2/s and an ADC ratio of 0.70.

Figure 3. ROC curves for differentiating malignant RIST from RT using latency, tumor volume, ADC_min, and ADC ratio. Malignant RIST is associated with longer latency, larger tumor volume, and higher ADC_{min} and ADC ratio compared with RT.

Figure 4. Flowchart to differentiate RIST from RT using MRI

Table 1 Clinical characteristics of patients who had secondary tumors following cranial irradiation for pediatric primary posterior fossa tumors

Patient No.	Age (y/o)	Sex	Primary tumor	Primary location	Secondary tumor	Secondary location	Latency (month)	F/u period (month)
1	6	F	Medulloblastoma	4th ventricle	Meningioma	Left superior parietal lobe	259	260*
2	5	F	Medulloblastoma	4th ventricle	Meningioma	Right high frontal lobe	258	466
3	9	F	Medulloblastoma	4th ventricle	Astrocytoma	Right basal ganglia	246	272*
4	9	M	Medulloblastoma	Right cerebellar hemisphere	GBM	Right basal ganglia and frontal lobe	49	55*
5	9	M	Medulloblastoma	4th ventricle	GBM	Left cerebellar hemisphere	115	119*
6	5	M	Medulloblastoma	4th ventricle	Meningioma	Right temporal lobe	222	224*
7	10	M	Medulloblastoma	Right cerebellar hemisphere	Olfactory neuroblastoma	Right frontal base	249	345
8	5	F	Medulloblastoma	4th ventricle	Meningioma	Left frontal lobe	239	432*
9	12	F	Medulloblastoma	4th ventricle	Meningioma	Left parietal lobe	400	492
10	12	F	Medulloblastoma	4th ventricle	GBM	Right cerebellar hemisphere and pons	80	89*
11	14	F	Medulloblastoma	4th ventricle	Meningioma	Right frontal lobe	363	409*
12	14	F	Medulloblastoma	4th ventricle	GBM	Left cerebellar hemisphere	137	149*
13	7	F	Medulloblastoma	4th ventricle	Meningioma	Left temporal lobe	354	392
14	5	F	Medulloblastoma	Left cerebellar hemisphere	GBM	Left high frontal lobe	37	76*
15	2	F	Medulloblastoma	4th ventricle	Trigeminal schwannoma	Right Meckel's cave	96	205
16	9	F	ATRT	Right cerebellar hemisphere	Osteosarcoma	Right occipital skull	34	64*
17	5	F	ATRT	4th ventricle	Malignant spindle cell tumor	Right frontal lobe	79	245

18	1	M	ATRT	Midbrain	GBM	Right basal ganglia	78	89*
19	7	M	ATRT	Right cerebellar hemisphere	GBM	Left centrum semiovale	79	84*
20	3	M	Ependymoma	Left cerebellar hemisphere	Meningioma	Right high frontal lobe	168	356

GBM, Glioblastoma; ATRT, Atypical Teratoid/Rhabdoid Tumors

* Follow-up period from primary tumor diagnosis to expired

Table 2 Clinical findings in radiation induced secondary tumor (RIST) and recurrent tumor (RT) group

	RIST (n=20)	RT (n=20)	p Value
Primary tumor type (%)			0.21
Medulloblastoma	15 (75)	12 (60)	
ATRT	4 (20)	3 (15)	
Ependymoma	1 (5)	5 (25)	
Sex (%)			0.06
Male	6 (30)	13 (65)	
Female	14 (70)	7 (35)	
Primary tumor age (years) (median, range)	7 (1-14)	5.8 (1-18)	0.15
Latency (months) (median, range)	152.5 (34-400)	22 (1-191)	<0.001
Alive at last follow-up	7 (35)	3 (15)	0.15

GBM, Glioblastoma; ATRT, Atypical Teratoid/Rhabdoid Tumor

Table 3 MRI features of malignant radiation induced second tumor (RIST) compared with recurrent tumor (RT) group

	Benign RIST (n=9)	Malignant RIST (n=11)	RT (n=20)	*P**	*P***	*P****
Location (%)				0.001	0.003	1
Distant	9 (100)	11 (100)	8 (40)			
Tumor base	0 (0)	0 (0)	12 (60)			
Intra or extra-axial (%)				0.45	0.04	0.01
Extra-axial	8 (89)	3 (27)	9 (45)			
Intra-axial	1 (11)	8 (73)	11 (55)			
Margin (%)				0.64	<0.001	0.001
Well defined	9 (100)	3 (27)	3 (15)			
Poorly defined	0 (0)	8 (73)	17 (85)			
Tumor size (cm^3) (range)	2.35 (0.99-174.37)	23.39 (2.72-57.4)	5.17 (0.21-63.54)	0.004	0.62	0.007
T1 (%)				1	0.31	0.45
High	1 (11)	0 (0)	0 (0)			
Iso to low	8 (89)	11 (100)	20 (100)			
T2 (%)				0.7	0.11	0.07
High	2 (22)	8 (73)	12 (60)			
Iso to low	7 (78)	3 (27)	8 (40)			
Enhancement (%)				0.53	1	0.45
Good	8 (89)	11 (100)	18 (90)			
Faint to no	1 (11)	0 (0)	2 (10)			
Enhancement pattern (%)				0.32	<0.001	0.01
Homogenous	8 (89)	3 (27)	2 (10)			
Heterogenous	1 (11)	8 (73)	18 (90)			
Cystic component (%)	2 (22)	4 (36)	6 (30)	1	1	0.64
Perifocal edema (%)	1 (11)	2 (18)	2 (10)	0.6	1	1
No tumor seeding (%)	9 (100)	11 (100)	11 (55)	0.01	0.03	1
Hydrocephalus (%)	1 (11)	2 (18)	3 (15)	1	1	1
DWI (%)				0.32	1	0.59
High	8 (89)	8 (73)	18 (90)			
Iso to low	1 (11)	3 (27)	2 (10)			
ADC (%)				0.42	0.21	1
High	5 (56)	5 (45)	5 (25)			
Iso to low	4 (44)	6 (55)	15 (75)			
Restricted DWI (%)	4 (44)	6 (55)	15 (75)	0.13	0.21	1
[a] ADC_{min} (10^{-6} mm^2/s)	839 (197-1112)	821 (638-1392)	644 (64-1208)	0.02	0.06	0.9
[b] ADC ratio	1.15 (0.9-1.82)	1.08 (0.81-2.71)	0.96 (0.7-1.87)	0.04	0.03	0.97
[b] DWI ratio	1.22 (0.76-1.37)	1.48 (0.58-2.03)	1.43 (0.85-1.71)	0.68	0.01	0.16

*P** = malignant RIST vs RT

*P*** = benign RIST vs RT

*P**** = benign RIST vs malignant RIST

[a] One outlier in the benign RIST group and two in the RT group were excluded

[b] Tumor/contralateral white matter ratio

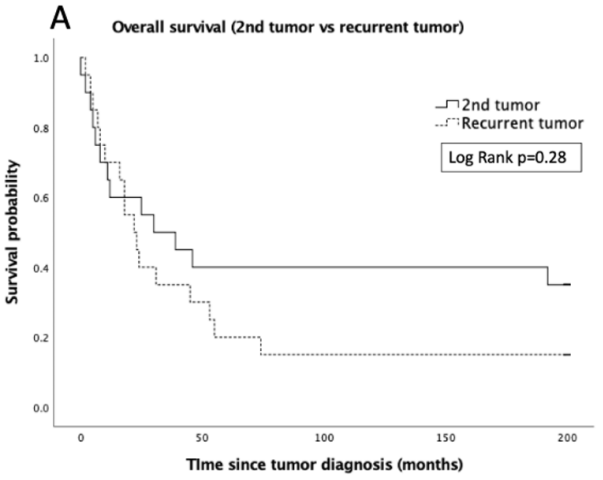

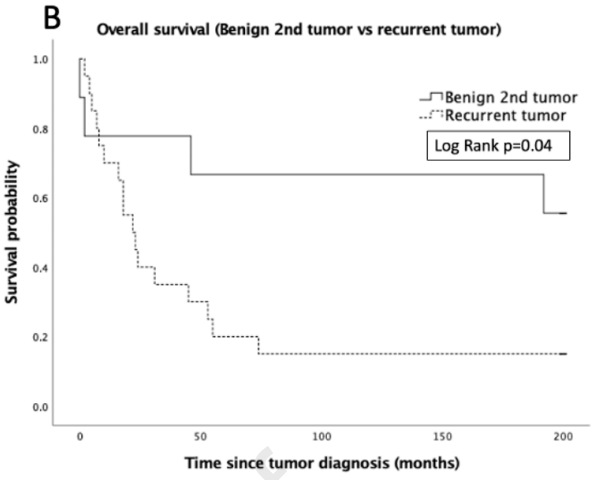

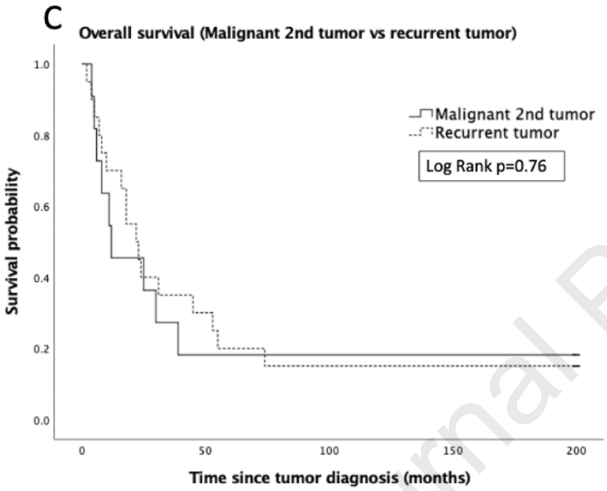

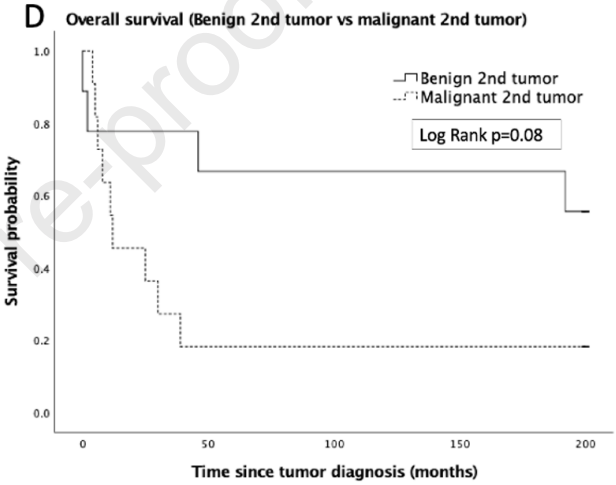

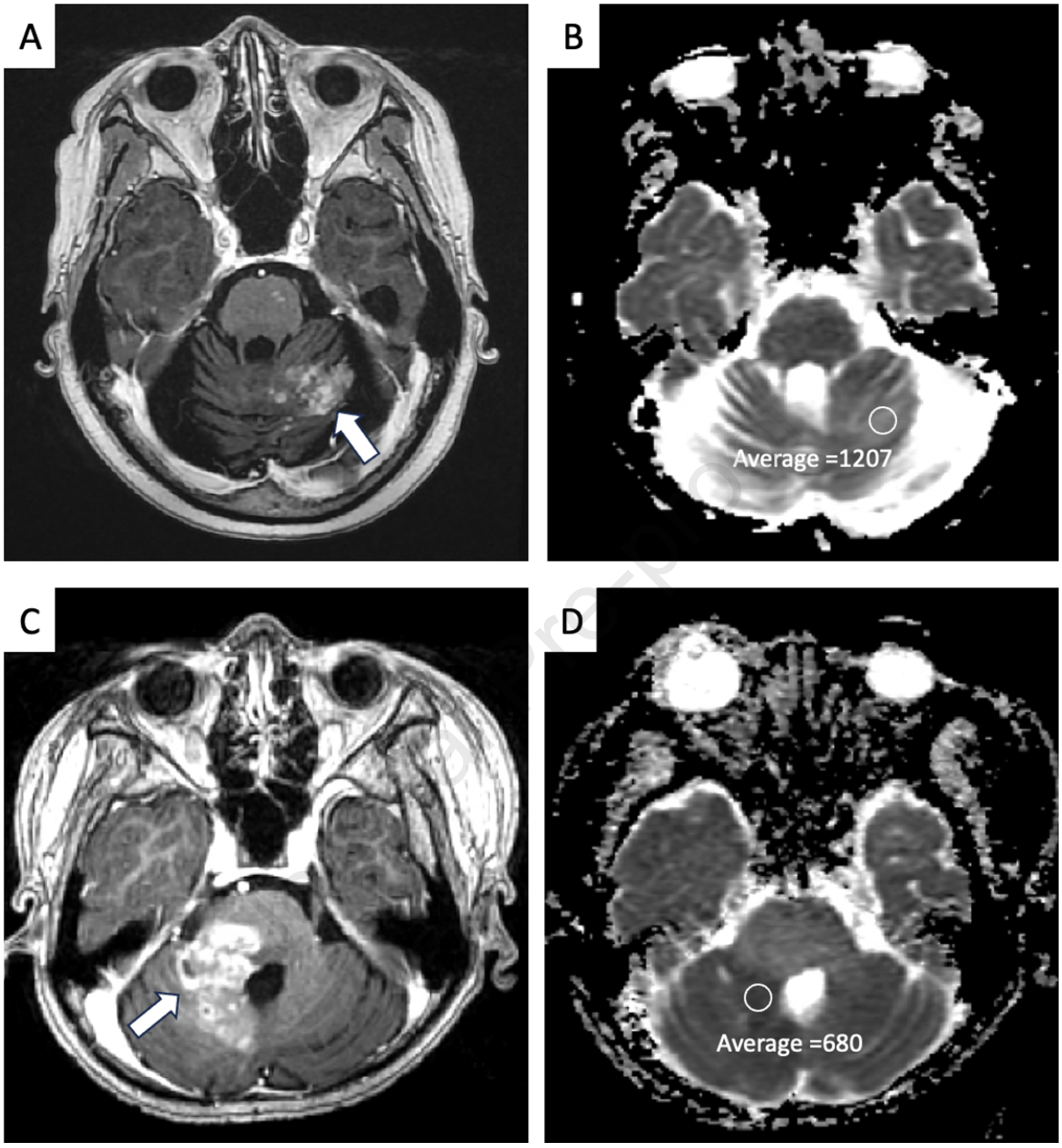
A
B
Average =1207
C
D
Average =680

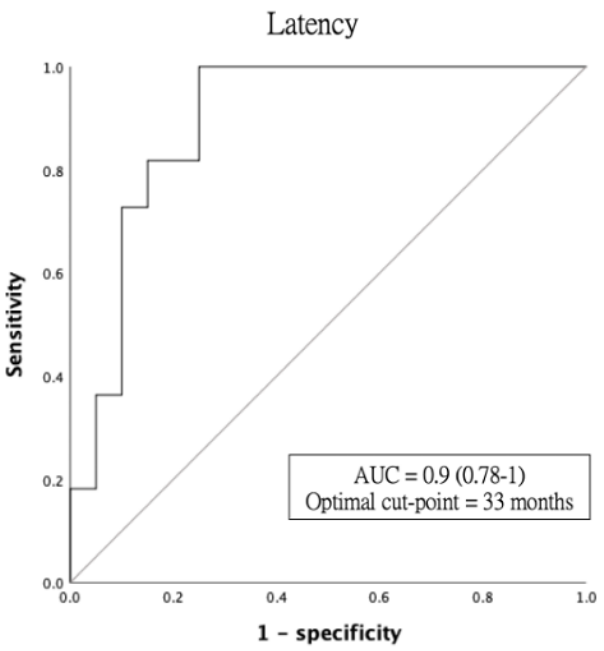

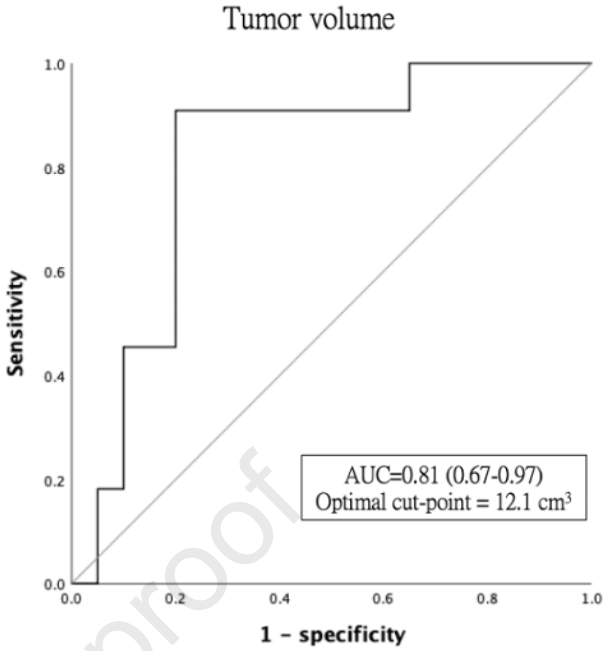

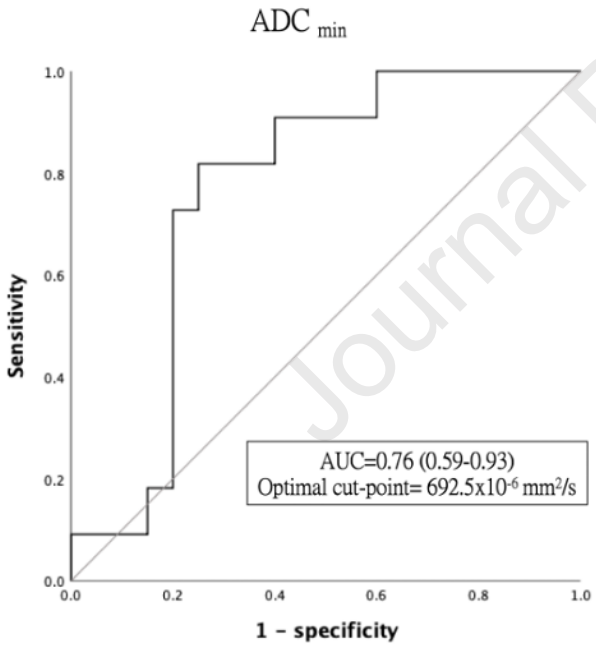

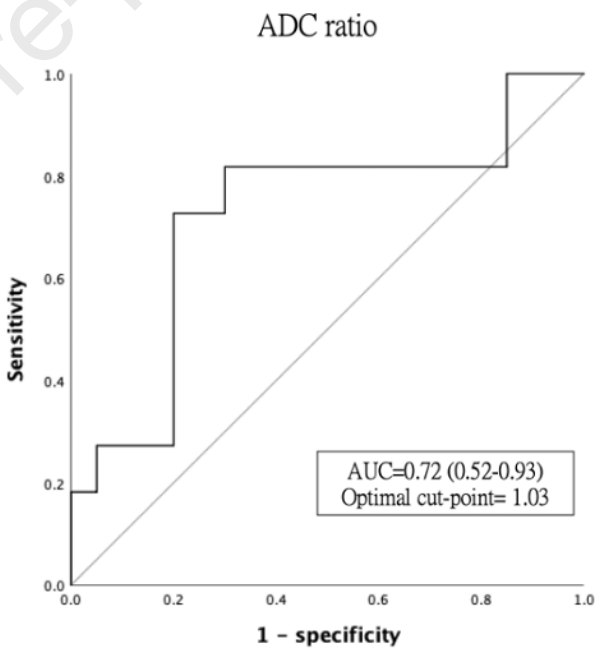

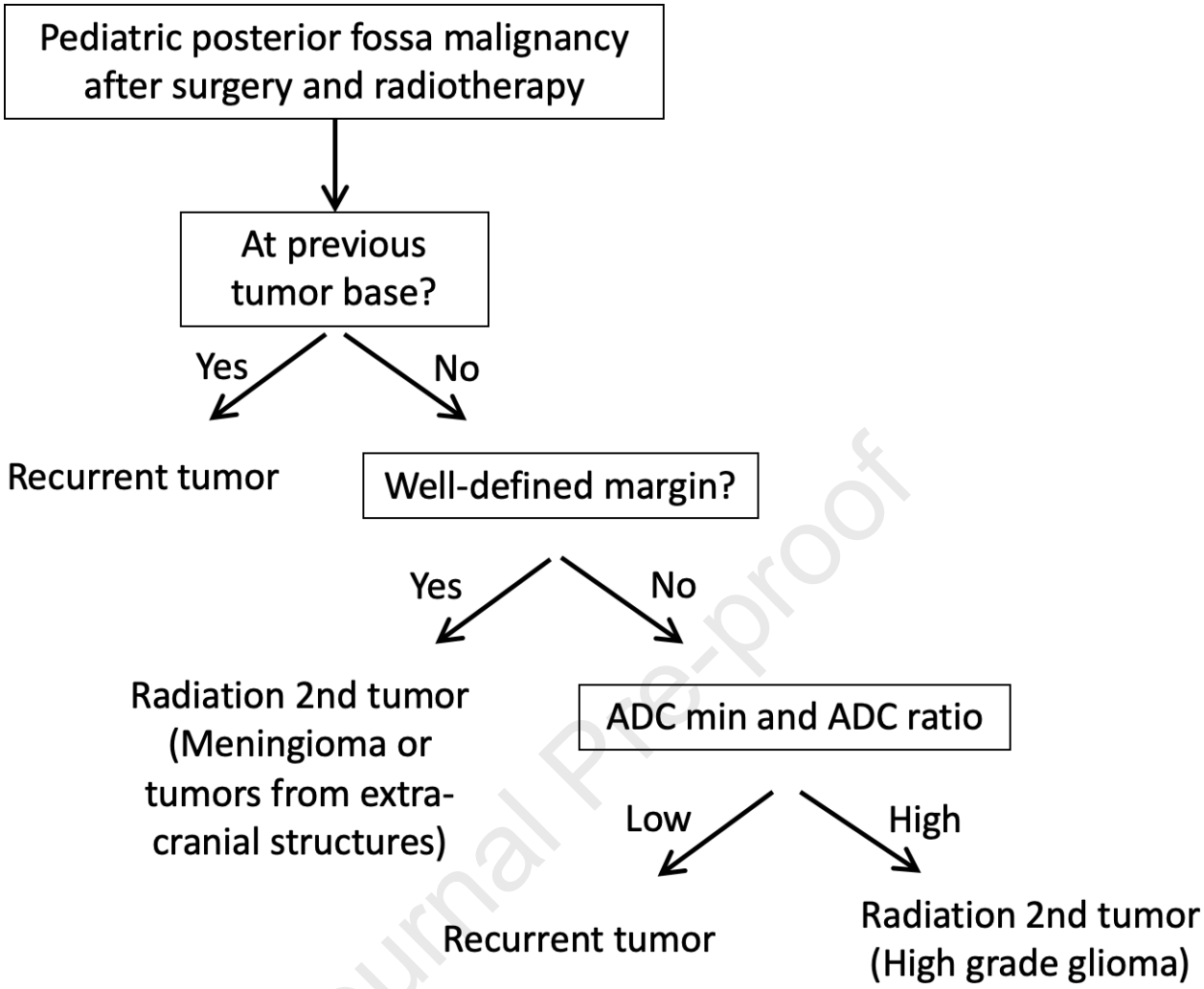

MPBTPF: malignant pediatric brain tumors of the posterior fossa

RIST: radiation-induced secondary tumor

RT: recurrent tumor

ATRT: atypical teratoid rhabdoid tumors

GBM: glioblastoma

DWI: Diffusion-weighted Imaging

ADC: apparent diffusion coefficient

SI: signal intensity

WI: weighted image

ROI: regions of interest

PACS: picture archiving and communication system

ORs: odds ratios

OS: overall survival

ROC: receiver operating characteristic

RIG: radiation-induced glioma

CSI: craniospinal irradiation

Conflict of Interest Statement:

The authors declare that they have no known competing financial interests or personal relationships that could have appeared to influence the work reported in this paper.